

# Symmetry constraints on phonon dispersion in graphene

L.A. Falkovsky<sup>1,2</sup>

<sup>1</sup>*L.D. Landau Institute for Theoretical Physics, Moscow 117334, Russia*

<sup>2</sup>*Institute of the High Pressure Physics, Troitsk 142190, Russia*

Taking into account the constraints imposed by the lattice symmetry, we calculate the phonon dispersion for graphene with interactions between the first, second, and third nearest neighbors in the framework of the Born–von Karman model. Analytical expressions obtained for the dispersion of the out-of-plane (bending) modes give the nonzero sound velocity. The dispersion of four in-plane modes is determined by coupled equations. Values of the force constants are found in fitting with frequencies at critical points and with elastic constants measured on graphite.

PACS numbers: 63.20.Dj, 81.05.Uw, 71.15.Mb

## I. INTRODUCTION

Since the pioneering experiments on graphene (a single atomic layer of graphite)<sup>1,2</sup>, main attention has been devoted to its electronic properties. More recently, Raman spectroscopy<sup>3</sup> extends to investigations of the lattice dynamics of graphene. It was found that the frequency ( $\approx 1590 \text{ cm}^{-1}$ ) of the Raman mode in graphene agrees with its value in graphite. Also, the overtone of the  $D$  mode visible almost in all carbon-consisting materials was observed at about  $2600 \text{ cm}^{-1}$ . However, this information is very meagre and does not provide a way to describe the lattice dynamics. The detailed knowledge of the lattice dynamics and electron-phonon interactions<sup>4</sup> is needed for interpretations of the Raman scattering as well as of the transport phenomena.

Several models<sup>5,6,7,8,9,10,11</sup> have been proposed to predict the phonon dispersion in graphene and bulk graphite from empirical force-constant calculations. A simplest approach assumes the diagonal form of the force-constant matrix which contains three constants for the interaction of an atom with all its  $n$ th-nearest neighbor. Thus, we meet 12 constants for graphene in the popular 4th-nearest neighbor approach or 15 constants in the 5th-nearest neighbor one<sup>12</sup>. The number of constants could be diminished if the model interactions are used<sup>13,14,15</sup> or if the phonon dispersion is considered only for the distinctive directions in the Brillouin zone<sup>16</sup>.

On the other hand, we can use the most recent results<sup>12,17,18,19,20,21</sup> of the first-principal calculations for the phonon dispersion in graphene and graphite. Comparison of that results for the high-frequency modes (see Table 1) shows disagreements as large as  $50 \text{ cm}^{-1}$  between the various approaches. The discrepancies could come either from an assumption that the force-constant matrix for the atom-neighbor interaction has a diagonal form or from an overestimation of the low-frequency modes. It is evident that atoms move more freely in out-of-plane direction in graphene than in graphite. Therefore, the frequencies of the out-of-plane mode in graphene should be less than the corresponding frequencies in graphite. Moreover, if the stiffness of the graphene layer is neglected, the dispersion of the acoustic out-of-plane

mode becomes quadratic as seen from the equation of elasticity (see also Ref.<sup>22</sup>). The interaction between layers in graphite can be estimated from the splitting of the low-frequency ZA and ZO' modes in graphite. One can see, for instance, from Ref.<sup>20</sup> that the value of the splitting is as much as  $130 \text{ cm}^{-1}$ . It means that (i) the result of graphene stiffness cannot be larger than that interaction and (ii) the agreement between the theory for graphene and the experimental low-frequency data for graphite cannot be better than about  $130 \text{ cm}^{-1}$ .

Here we present an analytical description of the phonon dispersion in graphene. This is done within the framework of the Born–von Karman model for the honeycomb graphene lattice including interactions only with first, second, and third nearest neighbors and taking the constraints imposed by the lattice symmetry into account. We show that the out-of-plane (bending) and in-plane modes are decoupled from each other. The out-of-plane modes are described by three force-constants determined in fitting with the Raman frequency and smallest elastic constant  $C_{44}$ . In the narrow wave-vector interval near the  $\Gamma$  point, the acoustic out-of-plane mode has a linear dispersion with the nonzero sound velocity. This means that a single graphene layer possesses the small but finite stiffness in contradiction with results of Ref.<sup>22</sup> We should emphasize that the quadratic dispersion of the acoustic mode leads to the large contribution (proportional to the sample size squared) of the long-range fluctuations, that is much stronger than the logarithmic function in the case of the linear dispersion. Six force-constants describing the in-plane modes are found in fitting with their frequencies in the critical points and elastic constants  $C_{11}$  and  $C_{12}$  of graphite.

## II. PHONON DYNAMICS IN NEAREST NEIGHBOR APPROXIMATION

The equations of motion in the harmonic approximation are written in the well-known form

$$\sum_{j,m,\kappa'} \Phi_{ij}^{\kappa\kappa'}(\mathbf{a}_n - \mathbf{a}_m) u_j^{\kappa'}(\mathbf{a}_m) = \omega^2 u_i^{\kappa}(\mathbf{a}_n), \quad (1)$$

where the vectors  $\mathbf{a}_n$  numerate the lattice cells, the superscripts  $\kappa, \kappa'$  note two sublattices  $A$  and  $B$ , and the subscripts  $i, j = x, y, z$  take three values corresponding to the space coordinates. Since the potential energy is the quadratic function of the atomic displacements  $u_i^A(\mathbf{a}_n)$  and  $u_i^B(\mathbf{a}_n)$ , the force-constant matrix can be taken in the symmetric form,  $\Phi_{ij}^{AB}(\mathbf{a}_n) = \Phi_{ji}^{BA}(-\mathbf{a}_n)$ , and its Fourier transform, i.e. the dynamical matrix, is a Hermitian matrix.

Each atom, for instance,  $\mathbf{A}_0$  (see Fig. 1) has three first neighbors in the other sublattice, *i.e.*  $B$ , with the relative vectors  $\mathbf{B}_1 = a(1, 0)$ ,  $\mathbf{B}_{2,3} = a(-1, \pm\sqrt{3})/2$ , where  $a = 1.42\text{\AA}$  is the carbon-carbon distance. The second neighbors are in the same sublattice  $A$  at distances  $\sqrt{3}a$  with the relative vectors  $\mathbf{A}_{1,4} = \pm a(0, \sqrt{3})$ ,  $\mathbf{A}_{2,5} = \pm a(-3, \sqrt{3})/2$ ,  $\mathbf{A}_{3,6} = \mp a(3, \sqrt{3})/2$ . The distance  $2a$  to the third neighbors  $\mathbf{B}'_1 = a(2, 0)$ ,  $\mathbf{B}'_{2,3} = a(1, \mp\sqrt{3})$  is slightly larger. The distance to the fourth neighbors is  $\sqrt{7}a = 2.65a$ . So, the difference between distances to the third and to fourth neighbors is nearly the same as the difference between distances to the first and to second ones. We will see that the force-constants become less by factor 5 while going from the first to the second neighbors (see Table 3). Therefore, we do not include the fourth neighbors into consideration.

For the first and third neighbors (in the  $B$  sublattice), the dynamical matrix has the form

$$\phi_{ij}^{AB}(\mathbf{q}) = \sum_{\kappa=1}^3 \Phi_{ij}^{AB}(\mathbf{B}_\kappa) \exp(i\mathbf{q}\mathbf{B}_\kappa) + \sum_{\kappa=1}^3 \Phi_{ij}^{AB}(\mathbf{B}'_\kappa) \exp(i\mathbf{q}\mathbf{B}'_\kappa), \quad (2)$$

and for the second neighbors (in the  $A$  sublattice)

$$\phi_{ij}^{AA}(\mathbf{q}) = \Phi_{ij}^{AA}(\mathbf{A}_0) + \sum_{\kappa=1}^6 \Phi_{ij}^{AA}(\mathbf{A}_\kappa) \exp(i\mathbf{q}\mathbf{A}_\kappa), \quad (3)$$

where  $\mathbf{A}_0$  indices the atom chosen at the center of the coordinate system in the  $A$  sublattice and the wave vector  $\mathbf{q}$  is taken in units of  $1/a$ .

The point group  $D_{6h}$  of the honeycomb lattice is generated by  $\{C_6, \sigma_v, \sigma_z\}$ , where  $\sigma_z$  is a reflection  $z \rightarrow -z$  by the plane that contains the graphene layer,  $C_6$  is a rotation by  $\pi/3$  around the  $z$  axis, and  $\sigma_v$  is a reflection by the  $xz$  plane. The transformations of the group impose constraints on the dynamical matrix. To obtain

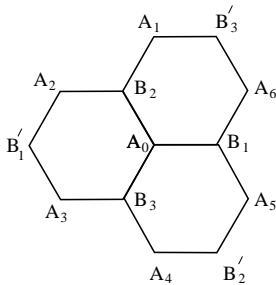


FIG. 1: First, second, and third neighbors in the graphene lattice.

them, we introduce variables  $\xi, \eta = x \pm iy$  transforming under the rotation  $C_3$  around the  $z$ -axis (taken at the  $\mathbf{A}_0$  atom) as follows  $(\xi, \eta) \rightarrow (\xi, \eta) \exp(\pm 2\pi i/3)$ . In the rotation, the atoms change their positions  $\mathbf{B}_1 \rightarrow \mathbf{B}_2 \rightarrow \mathbf{B}_3$ ,  $\mathbf{A}_1 \rightarrow \mathbf{A}_3 \rightarrow \mathbf{A}_5$ , and  $\mathbf{A}_2 \rightarrow \mathbf{A}_4 \rightarrow \mathbf{A}_6$ . Therefore, all the force constants  $\Phi_{\xi\eta}^{AB}(\mathbf{B}_\kappa)$  with the different  $\kappa$  (as well as  $\Phi_{zz}^{AB}(\mathbf{B}_\kappa)$ ) are equal to one another, but the force constants with the coincident subscripts  $\xi$  or  $\eta$  transform as covariant variables. For instance,  $\Phi_{\xi\xi}^{AB}(\mathbf{B}_1) = \Phi_{\xi\xi}^{AB}(\mathbf{B}_2) \exp(2\pi i/3) = \Phi_{\xi\xi}^{AB}(\mathbf{B}_3) \exp(-2\pi i/3)$ .

The relation between  $\Phi_{\xi\xi}^{AA}(\mathbf{A}_\kappa)$  with the points  $\mathbf{A}_1, \mathbf{A}_3, \mathbf{A}_5$  (and also between  $\mathbf{A}_4, \mathbf{A}_2, \mathbf{A}_6$ ) has the same form. The constants  $\alpha_z = \Phi_{zz}^{AB}(\mathbf{B}_1)$ ,  $\gamma_z = \Phi_{zz}^{AA}(\mathbf{A}_1)$ ,  $\alpha'_z = \Phi_{zz}^{AB}(\mathbf{B}'_1)$ ,  $\alpha = \Phi_{\xi\eta}^{AB}(\mathbf{B}_1)$ ,  $\alpha' = \Phi_{\xi\eta}^{AB}(\mathbf{B}'_1)$ , and  $\gamma = \Phi_{\xi\eta}^{AA}(\mathbf{A}_1)$  are evidently real. The constant  $\beta = \Phi_{\xi\xi}^{AB}(\mathbf{B}_1)$  as well as  $\beta' = \Phi_{\xi\xi}^{AB}(\mathbf{B}'_1)$  is real because the reflection  $(x, y) \rightarrow (x, -y)$  with  $\mathbf{B}_1 \rightarrow \mathbf{B}_1$ ,  $\mathbf{B}'_1 \rightarrow \mathbf{B}'_1$  belongs to the symmetry group. Besides, we have one complex force constant  $\delta = \Phi_{\xi\xi}^{AA}(\mathbf{A}_1)$ .

Two force constants  $\Phi_{zz}^{AA}(\mathbf{A}_0)$  and  $\Phi_{\xi\eta}^{AA}(\mathbf{A}_0)$  for the atom  $\mathbf{A}_0$  can be excluded in the ordinary way with the help of conditions imposed by invariance with respect to the translations of the layer as a whole in the  $x/z$  directions. Using the equations of motion (1) and Eqs. (2), (3), we find this stability condition  $\Phi_{\xi\eta}^{AA}(\mathbf{A}_0) + 6\Phi_{\xi\eta}^{AA}(\mathbf{A}_1) + 3\Phi_{\xi\eta}^{AB}(\mathbf{B}_1) + 3\Phi_{\xi\eta}^{AB}(\mathbf{B}'_1) = 0$  and the similar form for the  $zz$  components.

### A. Dispersion of bending out-of-plane modes

The out-of-plane vibrations  $u_z^A, u_z^B$  in the  $z$  direction are not coupled with the in-plane modes because the force constants of type  $\Phi_{xz}$  or  $\Phi_{yz}$  equals zero due to the reflection  $z \rightarrow -z$ . The corresponding dynamical matrix for the out-of-plane modes has the form

$$\begin{pmatrix} \phi_{zz}^{AA}(\mathbf{q}) & \phi_{zz}^{AB}(\mathbf{q}) \\ \phi_{zz}^{AB}(\mathbf{q})^* & \phi_{zz}^{AA}(\mathbf{q}) \end{pmatrix}, \quad (4)$$

where

$$\begin{aligned} \phi_{zz}^{AA}(\mathbf{q}) &= -3(\alpha_z + \alpha'_z) \\ &+ 2\gamma_z [\cos(\sqrt{3}q_y) + 2 \cos(3q_x/2) \cos(\sqrt{3}q_y/2) - 3], \\ \phi_{zz}^{AB}(\mathbf{q}) &= \alpha_z [\exp(iq_x) + 2 \exp(-iq_x/2) \cos(\sqrt{3}q_y/2)] \\ &+ \alpha'_z [\exp(-2iq_x) + 2 \exp(iq_x) \cos(\sqrt{3}q_y)]. \end{aligned} \quad (5)$$

The phonon dispersion for the out-of-plane modes is found

$$\omega_{ZO, ZA}(\mathbf{q}) = \sqrt{\phi_{zz}^{AA}(\mathbf{q}) \pm |\phi_{zz}^{AB}(\mathbf{q})|}. \quad (6)$$

The equations allow us to express the phonon frequencies of the out-of-plane branches at the critical points  $\Gamma, K$ ,

TABLE I: Force constants in  $10^5 \text{ cm}^{-2}$ :  $\alpha$ ,  $\beta$ , and  $\alpha_z$  for the first neighbors;  $\gamma$ ,  $\delta$ , and  $\gamma_z$  for the second neighbors;  $\alpha'$ ,  $\alpha'_z$ , and  $\beta'$  for the third neighbors.

$\alpha$	$\beta$	$\gamma$	$\delta$	$\alpha'$	$\beta'$	$\alpha_z$	$\gamma_z$	$\alpha'_z$
-4.095	-1.645	-0.209	0.690	-0.072	0.375	-1.415	0.171	0.085

and  $M$  in terms of the force constants:

$$\begin{aligned}\omega_{\text{ZO}}(\Gamma) &= [-6(\alpha_z + \alpha'_z)]^{1/2} \\ \omega_{\text{ZO, ZA}}(K) &= [-3(\alpha_z + \alpha'_z) - 9\gamma_z]^{1/2} \\ \omega_{\text{ZO}}(M) &= [-4\alpha_z - 8\gamma_z]^{1/2} \\ \omega_{\text{ZA}}(M) &= [-2\alpha_z - 6\alpha'_z - 8\gamma_z]^{1/2}.\end{aligned}\quad (7)$$

Expanding Eq. (6) in powers of the wave vector  $\mathbf{q}$ , we find the velocity of the acoustic out-of-plane mode propagating in the layer

$$s_z = a[-0.75\alpha_z - 3\alpha'_z - 4.5\gamma_z]^{1/2} = \sqrt{C_{44}/\rho}, \quad (8)$$

where we use the well-known formula for the velocity of the acoustic  $z$ -mode propagating in the  $x$ -direction in terms of the elastic constant  $C_{44}$  and density  $\rho$  of a hexagonal crystal. Because the interaction between the layers in graphite is weak, we can correspond the values of  $C_{44}$  and  $\rho$  to graphite.

## B. Dispersion of in-plane modes

The dynamical matrix for the in-plane vibrations has the form similar to that for the in-plane mode (4), but instead of the functions  $\phi_{zz}^{AA}(\mathbf{q})$  and  $\phi_{zz}^{AB}(\mathbf{q})$  we have to substitute correspondingly the  $2 \times 2$  matrices

$$\begin{pmatrix} \phi_{\xi\eta}^{AA}(\mathbf{q}) & \phi_{\xi\xi}^{AA}(\mathbf{q}) \\ \phi_{\xi\xi}^{AA}(\mathbf{q})^* & \phi_{\xi\eta}^{AA}(\mathbf{q}) \end{pmatrix}, \begin{pmatrix} \phi_{\xi\eta}^{AB}(\mathbf{q}) & \phi_{\xi\xi}^{AB}(\mathbf{q}) \\ \phi_{\eta\eta}^{AB}(\mathbf{q}) & \phi_{\xi\eta}^{AB}(\mathbf{q}) \end{pmatrix}. \quad (9)$$

The matrix elements  $\phi_{\xi\eta}^{AA}(\mathbf{q})$  and  $\phi_{\xi\eta}^{AB}(\mathbf{q})$  are obtained from  $\phi_{zz}^{AA}(\mathbf{q})$  and  $\phi_{zz}^{AB}(\mathbf{q})$ , Eqs. (5), correspondingly, with substitutions  $\gamma$ ,  $\alpha$ , and  $\alpha'$  instead of  $\gamma_z$ ,  $\alpha_z$ , and  $\alpha'_z$ . The off-diagonal elements are given by

$$\begin{aligned}\phi_{\xi\xi}^{AA}(\mathbf{q}) &= \\ &\delta[\exp(i\sqrt{3}q_y) + 2\cos(3q_x/2 + 2\pi/3)\exp(-i\sqrt{3}q_y/2)] + \\ &\delta^*[\exp(-i\sqrt{3}q_y) + 2\cos(3q_x/2 - 2\pi/3)\exp(i\sqrt{3}q_y/2)], \\ \phi_{\xi\xi}^{AB}(\mathbf{q}) &= \\ &\beta[\exp(iq_x) + 2\exp(-iq_x/2)\cos(\sqrt{3}q_y/2 - 2\pi/3)] \\ &+ \beta'[\exp(-2iq_x) + 2\exp(iq_x)\cos(\sqrt{3}q_y + 2\pi/3)].\end{aligned}$$

The matrix elements for the  $B$  sublattice can be obtained from that for the  $A$  sublattice by  $C_2$  rotation  $(x, y) \rightarrow -(x, y)$  of the graphene symmetry group. The optical

TABLE II: Elastic constants (in 10 GPa) and the sound velocities (in km/s) calculated (theo) and observed (exp).

	$C_{11}$	$C_{12}$	$C_{44}$	$s_{\text{LA}}$	$s_{\text{TA}}$	$s_z$
theo	86	18	0.57	19.5	12.2	1.59
exp	$106 \pm 2^a$	$18 \pm 2^a$	$0.45 \pm .05^a$	$\approx 24^b$	$14^b$	

<sup>a</sup> Reference<sup>23</sup>, <sup>b</sup> Reference<sup>24,25</sup>,

phonon frequencies for the in-plane branches at  $\Gamma$  and  $K$  are found

$$\begin{aligned}\omega_{1,2}^{\text{in-pl}}(\Gamma) &= [-6(\alpha + \alpha')]^{1/2}, \quad \text{doublet}, \\ \omega_{1,2}^{\text{in-pl}}(K) &= [-3(\alpha + \alpha') - 9\gamma]^{1/2}, \quad \text{doublet}, \\ \omega_{3,4}^{\text{in-pl}}(K) &= [-3(\alpha + \alpha') - 9\gamma \pm 3(\beta + \beta')]^{1/2}.\end{aligned}\quad (10)$$

An algebraic equation of the fourth order have to be solved in order to find the phonon frequencies at the  $M$  point as well as at points of the general position.

The in-plane vibrations make a contribution into the elastic constants  $C_{11}$  and  $C_{12}$ . The corresponding relation between the dynamic matrix elements and the elastic constants can be deduced taking the long-wavelength limit ( $\mathbf{q} \rightarrow 0$ ) in the matrices (9). In this limit, separating the acoustic vibrations  $\mathbf{u}^{\text{ac}}$  from the optical modes, we obtain the equation of motion in the matrix form

$$\begin{aligned} & [(\phi^{AA} + \phi^{AB} + \phi^{BB} + \phi^{BA})/2 \\ & + \phi_1^{AB}(\phi_0^{AB})^{-1}\phi_1^{AB} - \omega^2] \mathbf{u}^{\text{ac}} = 0, \end{aligned}\quad (11)$$

where the subscripts 0 and 1 mean that the terms of the zero and first order in  $\mathbf{q}$  should, correspondingly, be kept in the matrices (9), but the expansion to the second order is used in other terms. We find the matrix factor of  $\mathbf{u}^{\text{ac}}$

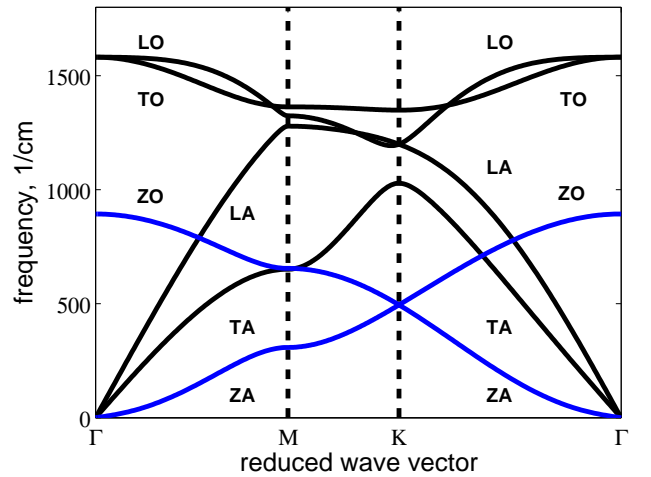


FIG. 2: Calculated phonon dispersion for graphene; the force constants, elastic constants, and phonon frequencies at critical points are listed in Tables 1, 2, and 3 correspondingly.

TABLE III: Phonon frequencies at critical points in  $\text{cm}^{-1}$ ;  $z$  and  $\parallel$  stand for the out-of-plane and in-plane branches, respectively.

	$\Gamma$ [0 0]		$M$ $[1 \sqrt{3}]\pi/3a$						$K$ $[0 1]4\pi/3\sqrt{3}a$			
	$\omega^\parallel$	$\omega^z$	$\omega_1^\parallel$	$\omega_2^\parallel$	$\omega_3^\parallel$	$\omega_4^\parallel$	$\omega_1^z$	$\omega_2^z$	$\omega_1^\parallel$	$\omega_{2,3}^\parallel$	$\omega_4^\parallel$	$\omega_{1,2}^z$
exp	1590 <sup>a</sup>	861 <sup>a</sup>	1389 <sup>a</sup>			630 <sup>d</sup>	670 <sup>a</sup>	471 <sup>c</sup>	1313 <sup>d</sup>	1184 <sup>b</sup>		482 <sup>d</sup>
	1583 <sup>b</sup>	868 <sup>c</sup>	1390 <sup>b</sup>	1323 <sup>b</sup>	1290 <sup>b</sup>			451 <sup>d</sup>	1265 <sup>b</sup>	1194 <sup>b</sup>		517 <sup>d</sup>
	1565 <sup>b</sup>	868 <sup>e</sup>				625 <sup>e</sup>	625 <sup>e</sup>	480 <sup>e</sup>	1285 <sup>e</sup>		1021 <sup>e</sup>	537 <sup>e</sup>
theo <sup>f</sup>	1595	890	1442	1380	1339	636	618	475	1371	1246	994	535
theo <sup>b</sup>	1581		1425	1350	1315				1300	1220		
theo	1581	893	1363	1324	1279	651	655	308	1349	1199	1028	495

<sup>a</sup> Reference<sup>16</sup>, <sup>b</sup> Reference<sup>19</sup>, <sup>c</sup> Reference<sup>6</sup>, <sup>d</sup> Reference<sup>26</sup>, <sup>e</sup> Reference<sup>12</sup>, <sup>f</sup> Reference<sup>17</sup>

in Eqs. (11):

$$\begin{pmatrix} s_1 q^2 - \omega^2 & s_2 q_+^2 \\ s_2 q_-^2 & s_1 q^2 - \omega^2 \end{pmatrix}, \quad (12)$$

where

$$s_1 = -\frac{9}{2}\gamma - \frac{3}{4}\alpha - 3\alpha' + \frac{3}{8}(\beta - 2\beta')^2/(\alpha + \alpha'),$$

$$s_2 = \frac{9}{4}\text{Re}(\delta) - \frac{3}{8}\beta - \frac{3}{2}\beta'.$$

With the help of Eq. (12), we obtain the velocities of longitudinal and transverse acoustic in-plane modes

$$s_{\text{LA}} = a\sqrt{s_1 + s_2} = \sqrt{C_{11}/\rho}, \quad (13)$$

$$s_{\text{TA}} = a\sqrt{s_1 - s_2} = \sqrt{(C_{11} - C_{12})/2\rho},$$

corresponding them to the elastic constants  $C_{11}$ ,  $C_{12}$  and density  $\rho$  of graphite.

### III. RESULTS AND DISCUSSIONS

The calculated phonon dispersion is shown in Fig. 2. Notice, first, that the sound velocities (for long waves,  $q \rightarrow \Gamma$ ) are isotropic in the  $xy$  plane as it should be appropriate for the symmetry of graphene. Second, the in-plane LO/TO modes at  $\Gamma$ , the in-plane LO/LA modes at  $K$ , and the out-of-plane ZA/ZO modes at  $K$  are doubly degenerate because graphene is the non-polar crystal and the  $C_{3v}$  symmetry of these points in the Brillouin zone admits the two-fold representation (observation of splitting of that modes in graphene would display the symmetry braking of the crystal).

Because of the lack of information on graphene, we compare the present theory with experiments on graphite. Thus, we have only three force constants  $\alpha_z$ ,  $\gamma_z$ , and  $\alpha'_z$  to fit four frequencies of the out-of-plane modes at the critical points  $\Gamma$ ,  $M$ , and  $K$ . We must keep in mind that the frequencies in graphene for the out-of-plane branches could be less than their values in graphite since the atoms are more free to move in the  $z$  direction in graphene comparatively with graphite. It is evident that the adjacent layers in graphite affect the low frequencies more intensively. The interaction of the

adjacent layers can be estimated from the ZA – ZO' splitting about  $130 \text{ cm}^{-1}$  given, for instance, in Ref.<sup>20</sup>. These modes become degenerate when the inter-layer interaction is switched off. Therefore, the lowest frequencies of out-of-plane modes calculated at the  $M$  and  $K$  points are considerably less than the corresponding frequencies observed in graphite (see Table 3).

Furthermore, the force constants determine the velocity  $s_z$ , Eq. (8), of the acoustic out-of-plane mode along with the elastic constant  $C_{44}$ . We see that the velocity has the nonzero value unless a definite condition is satisfied for the force constants. Using the values of force constants obtained in fitting with the experimental data (see Table 1), we find the value of the sound velocity  $s_z = 1.59 \text{ km/s}$  for the out-of-plane mode. This result is contradictory to the statement of Ref.<sup>22</sup> that the acoustic out-of-plane mode has a quadratic dispersion. The fact that the sound velocity  $s_z$  is very sensitive to the small variation of  $\gamma_z$  indicates that graphene is nearly unstable with respect to transformation into a phase of the lower symmetry group at  $\Gamma$ .

For the in-plane modes, we have to fit eight frequencies at the critical points and two elastic constants. Equations (10) and (13) can be used as a starting point. Fitting of the in-plane branches is insensitive to the imaginary part of the constant  $\delta$ . Therefore, it is taken as a real parameter. Results of the fit are presented in Fig. 2 and Tables. Notice, that the extent of agreement of the present theory with the data obtained for graphite corresponds to the comparison level between the first-principle calculations for graphite in Ref.<sup>19</sup> and their experimental data (see Table 3). The largest disagreement of 5% between our calculations and experiments on graphite for the highest phonon mode occurs at the  $K$  point. This is result of the Kohn anomaly due to the electron–phonon interaction<sup>27</sup> which reduces the phonon frequency at  $K$ . The same reason explains some overbending observed probably in graphite along the  $\Gamma - M$  direction.

### IV. CONCLUSIONS

We calculate the phonon dispersion in graphene using the Born–von Karman model with the first-, second-,

and third-neighbor interactions imposed by the symmetry constraints. The bending (out-of-plane) modes are not coupled with the in-plane branches and indicate the latent instability of graphene with respect to transformation into a lower-symmetry phase. The acoustic ZA mode has the linear dispersion in a small wave-vector interval near the  $\Gamma$  point. The optical frequencies of these modes are less than the corresponding values in graphite. For the higher in-plane modes, the fit shows good agreement

between the experimental and calculated values of optical frequencies, elastic constants, and acoustic velocities.

### Acknowledgments

The work was supported by the Russian Foundation for Basic Research (grant No.07-02-00571).

- 
- <sup>1</sup> K.S. Novoselov, A.K. Geim, S.V. Morozov et al., *Science*, **306**, 666 (2004); K.S. Novoselov et al., *Nature*, **438**, 197 (2005).
- <sup>2</sup> Y. Zhang, J.P. Small, M.E.S. Amory, and P.Kim, *Phys. Rev. Lett.* **94**, 176803 (2005).
- <sup>3</sup> C.C. Ferari, J.C. Meyer, V. Scardaci, C. Caseraghi, M. Lazzeri, F. Mauri, S. Piscanec, D. Jiang, K.S. Novoselov, S. Roth, and A.K. Geim, *Phys. Rev. Lett.* **97**, 187401 (2006).
- <sup>4</sup> A.H. Castro Neto, F. Guinea, *Phys. Rev. B* **75**, 045404 (2007).
- <sup>5</sup> J. De Launay, *Solid State Phys.* **3**, 203 (1957).
- <sup>6</sup> R. Nicklow, W. Wakabayashi, and H.G. Smith, *Phys. Rev. B* **5**, 4951 (1972).
- <sup>7</sup> A.A. Ahmadiéh and H.A. Rafizadeh, *Phys. Rev. B* **7**, 4527 (1973).
- <sup>8</sup> A.P.P. Nicholson and D.J. Bacon, *J. Phys. C* **10**, 2295 (1977).
- <sup>9</sup> M. Maeda, Y. Kuramoto, and C. Horie, *J. Phys. Soc. Jpn. Lett.* **47**, 337 (1979).
- <sup>10</sup> R. Al-Jishi and G. Dresselhaus, *Phys. Rev. B* **26**, 4514 (1982).
- <sup>11</sup> H. Gupta, J. Malhotra, N. Rani, and B. Tripathi, *Phys. Rev. B* **33**, 7285 (1986).
- <sup>12</sup> M. Mohr, J. Maultzsch, E. Dobardžić, I. Milošević, M. Damnjanović, A. Bosak, M. Krish, and C. Thomsen, *Phys. Rev. B* **76**, 035439 (2007).
- <sup>13</sup> L. Lang, S. Doyen-Lang, A. Charlier, and M.F. Charlier, *Phys. Rev. B* **49**, 5672 (1994).
- <sup>14</sup> G. Benedek and G. Onida, *Phys. Rev. B* **47**, 16471 (1992).
- <sup>15</sup> C. Mapelli, C. Castiglioni, G. Zerbi, and K. Müllen, *Phys. Rev. B* **60**, 12710 (1999).
- <sup>16</sup> T. Aizava, R. Souda, S.Otani, Y. Ishizava, and C. Oshima, Y. Samiyosh, *Phys. Rev. B* **42**, 11469 (1990).
- <sup>17</sup> O. Dubay and G. Kresse, *Phys. Rev. B* **67**, 035401 (2003).
- <sup>18</sup> L. Wirtz and A. Rubio, *Solid State Commun.* **131**, 141 (2004).
- <sup>19</sup> J. Maultzsch, S. Reich, C. Thomsen, H. Reequardt, and P. Ordejon, *Phys. Rev. Lett.* **92**, 075501 (2004).
- <sup>20</sup> N. Mounet and N. Marzari, *Phys. Rev. B* **71**, 205214 (2005).
- <sup>21</sup> V.N. Popov and P. Lambin, *Phys. Rev. B* **73**, 085407 (2006).
- <sup>22</sup> R. Saito, G. Dresselhaus, and M.S. Dresselhaus, *Physical Properties of Carbon Nanotubes*, p. 170, (Imperial College Press, London, 2003).
- <sup>23</sup> *Graphite and Precursors*, ed. by P. Delhaes (Gordon and Breach, Australia, 2001), Chap. 6.
- <sup>24</sup> D. Sánchez-Portal, E. Artacho, J.M. Soler, A.Rubio, and P. Ordejón, *Phys. Rev. B* **59**, 12678 (1999).
- <sup>25</sup> C. Oshima, T. Aizava, R. Souda, Y. Ishizava, and Y. Samiyosh, *Solid. State. Commun.* **65**, 1601 (1988).
- <sup>26</sup> H. Yanagisawa, T. Tanaka, Y. Ishida, M. Matsue, E. Rokuta, S. Otani, and C. Oshima, *Surf. Interface Anal.* **37**, 133 (2005).
- <sup>27</sup> S. Piscanec, M. Lazzeri, F. Mauri, A.C. Ferrari, and J. Robertson, *Phys. Rev. Lett.* **93**, 185503 (2004).